

Selective adsorption in $^4\text{He-MgO}$ scattering

Massoud Mahgerefteh, David R. Jung, and Daniel R. Frankl

Department of Physics, The Pennsylvania State University, University Park, Pennsylvania 16802

(Received 19 May 1988; revised manuscript received 30 September 1988)

Helium scattering data from an *in situ* cleaved, oxygen-treated, room-temperature surface of MgO(100) are reported. The sharpness of the selective adsorption line shapes as well as the strength of the scattered beams indicate an improvement over previous studies on air-cleaved surfaces. Selective adsorption line shapes in azimuthal scans of the specular intensity at many closely spaced angles of incidence are presented. Analysis of the resonances at several reciprocal lattice vectors yielded binding energies of 5.52, 2.57, 1.16, 0.54, and 0.26 meV.

INTRODUCTION

Scattering of low-energy He atoms has been widely used to study gas-surface interaction potentials.¹⁻⁴ The phenomenon of bound-state resonance or "selective adsorption" provides accurate information about the interaction potential between the gas atom and crystal surface. Several alkali halide surfaces have been studied extensively by this method. Most other ionic crystals have received little attention, but one exception is MgO, for which four nozzle-beam experiments⁵⁻⁸ and one effusive-beam experiment⁹ have been reported. The four nozzle-beam studies all employed air-cleaved surfaces. The total coherently scattered intensity was weak (about 15% of the incident beam^{5,7}) while the incoherently scattered intensity was large compared to some of the alkali halides.⁶ Each of the nozzle-beam studies reported diffracted beam intensities and a corresponding value of the surface corrugation amplitude based on a hard corrugated wall surface model. Data on the bound-state energies of the He-MgO potential are rather scant. Cantini and Cevasco⁷ assumed a well depth of 8 meV based on preliminary observations of selective adsorption. Brusdeylins *et al.*⁶ reported bound-state energies of 10.2, 6.0, 2.6, and 1.2 meV and a well depth of 12.5 meV based on features interpreted as selective desorption in polar angle scans of near-specular intensity. Adsorption isotherm measurements of He on MgO smoke¹⁰ gave a ground-state level at 4.8 meV. We report here the first nozzle-beam study on a vacuum-cleaved MgO(100) surface. The sharpness of the selective adsorption line shapes as well as the strength of the scattered beams indicate an improvement over previous studies.

RESUME OF THEORY

For a perfect single-crystal surface the potential is a function of the distance coordinates parallel and perpendicular to the surface, and may be written as

$$V(\mathbf{r}) = V_0(z) + \sum_{\mathbf{G} \neq 0} V_{\mathbf{G}}(z) e^{i\mathbf{G} \cdot \mathbf{R}}, \quad (1)$$

where \mathbf{G} is a surface reciprocal-lattice vector and

$\mathbf{r} = (z, \mathbf{R})$ is the vector position of the atom above the surface. For certain incident conditions, the incident particle can be trapped in a discrete bound state with respect to motion perpendicular to the surface while being in a two-dimensional Bloch state with respect to motion parallel to the surface. When this occurs sharp minima and maxima appear in the elastic beam intensities.

The bound-state energies are the discrete solutions of the one-dimensional Schrödinger equation employing the potential in Eq. (1). Approximate solutions can be obtained by treating the periodic part, i.e., the summation, as a perturbation. Hence the unperturbed wave functions are of the form

$$\psi_{\nu, \mathbf{G}}(\mathbf{r}) = \phi_{\nu}(z) e^{i(\mathbf{K} + \mathbf{G}) \cdot \mathbf{R}}, \quad (2)$$

where \mathbf{K} is the part of the incident wave vector parallel to the surface and where ϕ_{ν} is a solution of

$$\left[- \left(\frac{\hbar^2}{2m} \right) \frac{d^2}{dz^2} + V_0(z) \right] \phi_{\nu}(z) = \epsilon_{\nu} \phi_{\nu}(z). \quad (3)$$

ϵ_{ν} is the (negative) energy of the ν th bound state of $V_0(z)$. Conservation of energy and crystal momentum then yield the relation

$$\left[\frac{2m}{\hbar^2} \right] \epsilon_{\nu} + (\mathbf{K} + \mathbf{G})^2 = \mathbf{k}^2, \quad (4)$$

where \mathbf{k} is the wave vector of the incident beam. From Eq. (4) a plot of the selective adsorption loci in the K_x - K_y plane should result in circles centered at $-\mathbf{G}$ and having radii $[k_i^2 - (2m/\hbar^2)\epsilon_{\nu}]^{1/2}$. This picture describes the positions of the resonances under conditions where there are no degeneracies (crossing of circles).

EXPERIMENTAL METHODS

The basic apparatus used has been described in detail elsewhere.¹¹ The beam is produced by expanding high-pressure He gas (≈ 600 psi) through a 5- μm nozzle at liquid-nitrogen temperature. This results in a beam which is quite monochromatic and of low energy ($k = 5.76 \text{ \AA}^{-1}$, $\lambda \approx 1 \text{ \AA}$). The beam-velocity spread is less

than 2% full width at half maximum (FWHM). The angular divergence $\Delta\theta$ is less than 10^{-3} rad and the beam width is about 1 mm at the sample in some runs and 0.5 mm in others. A few runs were also made with a room-temperature beam ($k = 11.0 \text{ \AA}^{-1}$).

The sample holder has two degrees of freedom so that the polar and azimuthal angles (denoted by θ and ϕ , respectively) can be varied independently. The face of the crystal can also be adjusted with respect to tilt and position along the azimuthal axis. The sample holder can be heated to 900 K or cooled to 25 K. A quadrupole mass spectrometer with a rectangular slit subtending an angle of 0.9° at the surface of the crystal, having motions in and perpendicular to the plane of incidence, is used as detector. The scattering chamber is maintained at a base pressure of 3×10^{-10} Torr, but during the experiment the pressure rises to low 10^{-9} Torr. The samples used in this work were rods ($8 \times 8 \times 25 \text{ mm}^3$) of MgO cleaved from boules obtained from unknown sources.

The crystal is outgassed at 900 K and then cleaved *in situ* at room temperature by a tungsten carbide blade on a bellows-sealed rod. Cleaves are highly variable in appearance and reflection intensity, but all appear macroscopically rough to some extent. Good cleaves give specular intensities as high as 35% of the incident beam, with line shapes showing no perceptible broadening. This initial intensity decays rapidly, in part due to stray electrons from the detector despite the absence of any line of sight from the filament to the sample. This effect was eliminated by negatively biasing the detector entrance plate at several hundred volts, but the specular intensity still decayed with a time constant of about 5 h. This deterioration could not be reversed by heating alone, but heating in oxygen (900 K, 10^{-8} Torr, 15 min) gave partial restoration. When the oxygen treatment was also given immediately after cleaving, surface deterioration was minimized, and specular intensities of order 20% could later be regained by repeating the treatment. The effect may be due in part to the removal of carbon contamination.¹² In any case, successive treatments became less and less effective, and after about four of them a new cleave was required.

The experiment consists of scanning of the azimuthal angle ϕ at fixed polar angle θ and monitoring the specular intensity to determine the angles at which the resonance features, sharp minima or maxima, occur. This is done for a range of polar angles, and the results give a map of the selective adsorption loci in the K_x - K_y plane.

RESULTS

The data presented here are all from one cleave. Other data taken more recently with a narrower beam and detector slit have confirmed the results. All of the experiments were done with the crystal at 300 K.

Azimuthal scans were recorded at 36 polar angles from 38° to 83° over a 4-d period with oxygen treatments in between. A sampling of these scans is shown in Fig. 1. The coordinates of all maxima and minima were plotted in the K_x - K_y plane, and only those which lay on or close to circles with centers at reciprocal-lattice points were taken to

be resonances. This accounted for nearly all features, although a few, mainly near the $0(0,1)$ and $0(1,1)$ circles, could not be unambiguously identified and were therefore omitted. The identified resonances were checked to ascertain that the character of each agreed with the prediction of Celli *et al.*¹³ based on the parity of the index,

$$l = \frac{1}{2}(|m| + |m' - m| - |m'| + |n| + |n' - n| - |n'|), \quad (5)$$

where m and n are the reciprocal-lattice indices of the resonance, and m' and n' those of the diffraction beam being monitored. Even or odd l indicates minima or maxima, respectively. A sample plot of selective adsorption loci in the K_x - K_y plane for the $\nu=0$ resonance level is shown in Fig. 2. Resonances with reciprocal-lattice

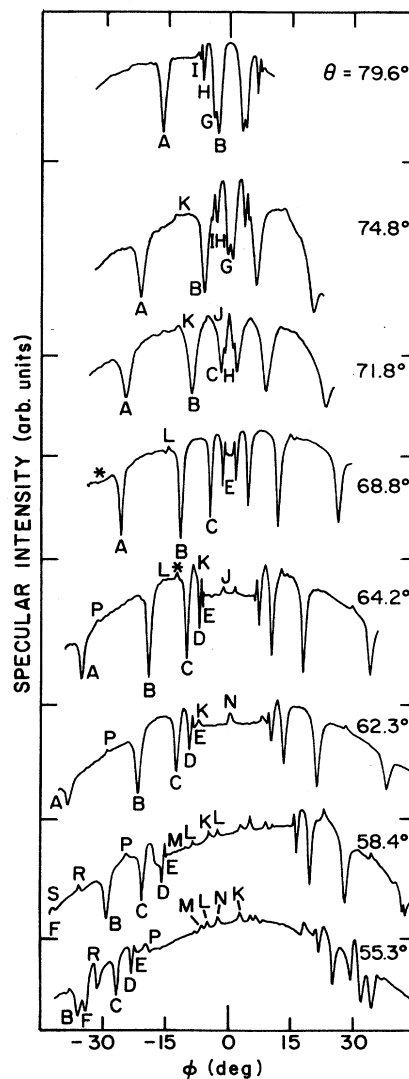


FIG. 1. Sampling of azimuthal scans of the specular intensity for an incident beam of ${}^4\text{He}$ ($k = 5.76 \text{ \AA}^{-1}$)/MgO(001). The curves are hand tracings of X-Y recorder charts. The labels identify the resonances according to Table I. Scale marks on the vertical axis are the zeros of the successive scans.

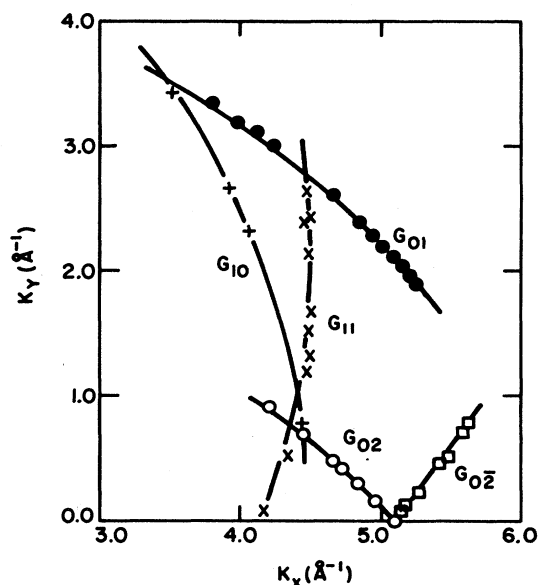


FIG. 2. Selective adsorption loci in the K plane for ${}^4\text{He}/\text{MgO}(001)$. Lines are circles described by Eq. (4), with $\nu=0$, and centered at G_{mn} . Radii are calculated in accordance with individual average energies as given in Table I.

vectors $(1,0)$, $(0,1)$, $(0,\bar{1})$, $(1,1)$, $(1,\bar{1})$, $(2,0)$, and $(0,\bar{2})$ were observed yielding five bound-state levels. The binding energies are determined via Eq. (4), and are shown with associated reciprocal-lattice vectors in Table I. Results with the room temperature beam in the range $70^\circ \leq \theta \leq 84^\circ$ are given in Table II.

An extensive search was made in all scans for resonances due to a deeper level as reported by Brusdeylins *et al.*,⁶ but none was found. Accordingly, we assign the index $\nu=0$ to the 5.5-meV level. The evidence for the absence of a deeper level is as follows.

(1) With the 77-K beam, the (01) resonance for a 10-meV level would be allowed for $\theta \geq 75^\circ$, ϕ near 45° . The (01) resonances found are all very strong minima (except for $\nu=4$). Scans up to $\theta=83^\circ$ showed no sign of any additional features of this type.

(2) With the 300-K beam this resonance would appear for $\theta \geq 70^\circ$. Again, the scans in this region showed no such feature.

(3) With either beam temperature the (10) resonance would appear in a narrow band of θ values, moving rapidly over the range $0^\circ \leq \phi \leq 45^\circ$. Two example locations are designated by the asterisks in Fig. 1. No distinct feature was seen in any of the scans. A weak minimum would be expected.

TABLE I. Selective adsorption bound state energies of ${}^4\text{He}/\text{MgO}(001)$. Incident-beam wave vector 5.76 \AA^{-1} .

Bound state	G_{mn}		Label ^a	Character	No. of points	Energy (meV)	
ν	m	n					
0	0	1	A	Deep min.	13	5.57 ± 0.08	5.52 ± 0.15^b
0	1	0	F	Deep min.	4	5.34 ± 0.03	
0	0	$\bar{2}$	J	Small max.	11	5.49 ± 0.13	
0	0	2	N	Small max.	8	5.62 ± 0.18	
0	1	$\bar{1}$	P	Small max.	10	5.50 ± 0.17	
0	1	1		Small max.	1	5.54	
1	0	1	B	Deep min.	15	2.51 ± 0.09	2.57 ± 0.15
1	0	$\bar{2}$	K	Small max.	16	2.65 ± 0.07	
1	0	2		Small max.	9	2.63 ± 0.1	
1	1	$\bar{1}$	R	Small max.	7	2.45 ± 0.18	
2	0	1	C	Deep min.	17	1.10 ± 0.08	1.16 ± 0.12
2	0	$\bar{1}$	G	Deep min.	3	0.99 ± 0.01	
2	0	$\bar{2}$	L	Small max.	18	1.22 ± 0.11	
2	0	2		Small max.	2	1.22 ± 0.09	
2	1	$\bar{1}$	S	Small max.	7	1.23 ± 0.13	
3	0	1	D	Deep min.	9	0.54 ± 0.02	0.54 ± 0.10
3	0	$\bar{1}$	H	Deep min.	5	0.42 ± 0.02	
3	0	$\bar{2}$	M	Small max.	10	0.55 ± 0.08	
3	0	2		Small max.	2	0.68 ± 0.03	
4	0	1	E	Small min.	7	0.27 ± 0.02	0.26 ± 0.03
4	0	$\bar{1}$	I	Small min.	3	0.21 ± 0.01	
4	0	$\bar{2}$		Small max.	3	0.28 ± 0.02	

^a Indicates the position of the resonances as shown in Fig. 1.

^b Weighted average.

TABLE II. Selective adsorption bound-state energies of $^4\text{He}/\text{MgO}(001)$. Incident-beam wave vector 11.0 \AA^{-1} .

Bound state ν	G_{mn}		Character	No. of points	Energy (meV)	
	m	n				
0	0	1	Deep min.	4	5.33±0.19	5.32±0.16
0	0	$\bar{2}$	Small max.	2	5.30±0.12	
1	0	1	Deep min.	4	2.62±0.17	2.62±0.14
1	0	$\bar{2}$	Small max.	2	2.63±0.04	
2	0	1	Deep min.	2	1.03±0.02	1.17±0.19
2	0	$\bar{1}$	Deep min.	2	1.32±0.16	
3	0	$\bar{1}$	Small min.	1	0.49	0.49

(4) In the case of the cold beam, the presence of the (10) resonance would also have greatly perturbed the $G_{\bar{1}\bar{1}}$ resonances which it would cross [e.g., the $0(1, \bar{1})$ at around $\theta=70^\circ$], since the coupling of these states is via the (01) Fourier component of the potential. Such effects are seen at the crossing of the $0(1,0)$ resonance with the $0(1, \bar{1})$, $1(1, \bar{1})$, and $2(1, \bar{1})$ resonances in the scans from 50° to 58° . The absence of any strong perturbation of the $(1, \bar{1})$ resonances above 58° is further evidence for the absence of a deeper level.

We have also measured the angular widths of several of these resonances. By the Heisenberg uncertainty principle, we have estimated the resonance lifetimes τ and the distance traveled along the surface L . These are given in Table III. L may be interpreted as a measure of the average distance between surface defects which scatter the atom out of resonance. A previous measurement on LiF gave similar results.¹⁴

ERROR ANALYSIS

Experimental error arises primarily from the difficulty in ascertaining the true incidence angles. The main problem in measuring θ is the determination of zero. The orientation of the gross surface envelope plane is easily found by maximizing the signal from a partially blocked beam. However, owing to the irregularity of the cleaved surface, there is no assurance that the local surface is parallel to this plane. Therefore, it is more reliable to

TABLE III. Half-widths and estimated lifetimes of bound-state resonances of $^4\text{He}/\text{MgO}(001)$. Incident beam wave vector 5.76 \AA^{-1} .

ν	$\Delta\phi$ (deg)	$\Delta\epsilon$ (meV)	τ (10^{-11} s)	L (\AA)
0	1.0	0.18	2.3	230
1	0.8	0.18	2.4	230
2	0.7	0.15	2.7	260
3	0.4	0.08	5.7	500
4	0.2	0.04	11.0	1000

measure θ from the detector angle. For this purpose, however, it is essential to have the crystal and detector axes collinear, the local surface tangent to this common axis, and the beam centered on it. These conditions are approximated by a lengthy series of adjustments with partially blocked beams. The resolution of the polar-angle measurements is about 0.1° .

The zero in the azimuthal angle is determined from the symmetry of the azimuthal reflection patterns. The procedure is to plot the intensity of the specular beam as a function of ϕ for fixed θ . Correct tilt of the crystal is verified when the specular intensity throughout a wide azimuthal scan is generally level. Our scans were made with a fixed detector position optimized at $\phi=0^\circ$. The scans show some dropoff of intensity at large ϕ due to residual tilt. The resolution for ϕ is about 0.3° .

The beam velocity is taken from previous measurements with a mechanical velocity selector.¹⁵ The value was later confirmed by precise diffraction measurements on graphite crystals. We were able to confirm it periodically by diffraction from the MgO crystals. We could also confirm that the beam temperature was fully down to liquid-nitrogen temperature by noting a slight shift of nozzle position when the cooler fills with liquid.

Differentiation of Eq. (4) yields estimates of the relative importance of errors in θ , ϕ , and k in determination of the binding energies.³ The error for each energy level is taken to be the sum of the magnitudes of the three individual errors evaluated in the region of the actual measured points. We find that $\Delta\epsilon_\nu \approx 0.15$ meV for all cases of interest. This roughly agrees with the statistical errors which are listed in the table; actual error may be greater.

DETERMINATION OF THE POTENTIAL

The depth D of the He/MgO(100) potential well was estimated by fitting the measured bound-state energy levels to the form of the potential given by Cole and Tsong,¹⁶

$$V(z) = (3^{3/2}D/2)[(\sigma/z)^9 - (\sigma/z)^3], \quad (6)$$

whose eigenvalues are given approximately by

$$|\epsilon_\nu| = D \left[1 - (\nu + \frac{1}{2})/L \right]^6, \quad (7)$$

where $L = (3.07/\pi)(2mD\sigma^2/\hbar^2)^{1/2}$. This two-parameter form is correct in the limit of large separation.¹⁶ Fitting the $|\epsilon_v|$ values to a sixth-power function gives $D = 7.5 \pm 0.2$ meV and $\sigma = 2.65 \pm 0.02$ Å. A least-squares fit of the $|\epsilon_v|^{1/6}$ values to a linear function gives nearly the same results. As is commonly found, the C_3 value is considerably larger than theoretical asymptotic limits.^{17,18}

DISCUSSION

The ground-state energy has been found to be 5.52 meV, in fair agreement with the He-MgO smoke adsorption measurements of Sullivan *et al.*,¹⁰ which gave a deepest bound-state level of 4.8 meV. Previous work on the He-graphite system has also shown a close agreement

between the results of atom-scattering and thermodynamic experiments.⁴ The 10.2-meV level reported by Brusdeylins *et al.*⁶ was not found, but if that level is given the alternate assignment of 1.2 meV, then their measured energy spectrum becomes quite similar to that found here.

Measurements of diffracted beam intensities are in progress.

ACKNOWLEDGMENTS

The authors thank the National Science Foundation for their support of this work under Grant Nos. DMR-84-19261 and DMR-87-18771. We would also like to thank Mr. Bradley Weaver and Professor M. W. Cole for helpful discussions.

¹D. R. Frankl, *Prog. Surf. Sci.* **13**, 285 (1983).

²W. Y. Leung, J. Z. Larese, and D. R. Frankl, *Surf. Sci.* **136**, 649 (1984).

³G. Derry, D. Wesner, S. V. Krishnaswamy, and D. R. Frankl, *Surf. Sci.* **74**, 245 (1978).

⁴M. W. Cole, D. R. Frankl, and D. L. Goodstein, *Rev. Mod. Phys.* **53**, 199 (1981).

⁵K. H. Rieder, *Surf. Sci.* **118**, 57 (1982).

⁶G. Brusdeylins, R. Bruce Doak, J. G. Skofronick, and J. Peter Toennies, *Surf. Sci.* **128**, 191 (1983).

⁷P. Cantini and E. Cevasco, *Surf. Sci.* **148**, 37 (1984).

⁸Eliezer Kolodney and Aviv Amirav, *Surf. Sci.* **155**, 715 (1985).

⁹R. Grant Rowe and Gert Ehrlich, *J. Chem. Phys.* **63**, 4648 (1975).

¹⁰Timothy S. Sullivan, Aldo D. Migone, and Oscar E. Vilches, *Surf. Sci.* **162**, 461 (1985).

¹¹S. Chung, A. Kara, J. Z. Larese, W. Y. Leung, and D. R. Frankl, *Phys. Rev. B* **35**, 4870 (1987); B. D. Weaver and D. R. Frankl, *Rev. Sci. Instrum.* **58**, 2115 (1987).

¹²R. Dale Moorhead and Helmut Poppa, *Thin Solid Films* **58**, 169 (1979).

¹³V. Celli, N. Garcia, and J. Hutchison, *Surf. Sci.* **87**, 112 (1979).

¹⁴G. Brusdeylins, R. Bruce Doak, and J. Peter Toennies, *J. Chem. Phys.* **75**, 1784 (1981).

¹⁵J. A. Meyers, Ph.D. thesis, The Pennsylvania State University, 1975.

¹⁶Milton W. Cole and T. T. Tsong, *Surf. Sci.* **69**, 325 (1977).

¹⁷Suckmin Chung and Milton W. Cole, *Surf. Sci.* **145**, 269 (1984).

¹⁸K. Nath, Z. W. Gortel, and H. J. Kreuzer, *Surf. Sci.* **155**, 596 (1985).